AGU PUBLICATIONS

Water Resources Research

RESEARCH ARTICLE
10.1002/2014WR016058

Analytical steady-state solutions for water-limited cropping systems using saline irrigation water

T. H. Skaggs[1], R. G. Anderson[1], D. L. Corwin[1], and D. L. Suarez[1]

[1]U.S. Salinity Laboratory, USDA-ARS, Riverside, California, USA

Key Points:
- The decreasing availability of water for irrigation requires improved management
- Models are presented that permit analyses of water-limited irrigated systems
- The models have several advantages over available alternatives

Correspondence to:
T. H. Skaggs,
todd.skaggs@ars.usda.gov

Citation:
Skaggs, T. H., R. G. Anderson, D. L. Corwin, and D. L. Suarez (2014), Analytical steady-state solutions for water-limited cropping systems using saline irrigation water, *Water Resour. Res.*, *50*, 9656–9674, doi:10.1002/2014WR016058.

Received 26 JUN 2014
Accepted 16 NOV 2014
Accepted article online 24 NOV 2014
Published online 26 DEC 2014

Abstract Due to the diminishing availability of good quality water for irrigation, it is increasingly important that irrigation and salinity management tools be able to target submaximal crop yields and support the use of marginal quality waters. In this work, we present a steady-state irrigated systems modeling framework that accounts for reduced plant water uptake due to root zone salinity. Two explicit, closed-form analytical solutions for the root zone solute concentration profile are obtained, corresponding to two alternative functional forms of the uptake reduction function. The solutions express a general relationship between irrigation water salinity, irrigation rate, crop salt tolerance, crop transpiration, and (using standard approximations) crop yield. Example applications are illustrated, including the calculation of irrigation requirements for obtaining targeted submaximal yields, and the generation of crop-water production functions for varying irrigation waters, irrigation rates, and crops. Model predictions are shown to be mostly consistent with existing models and available experimental data. Yet the new solutions possess advantages over available alternatives, including: (i) the solutions were derived from a complete physical-mathematical description of the system, rather than based on an ad hoc formulation; (ii) the analytical solutions are explicit and can be evaluated without iterative techniques; (iii) the solutions permit consideration of two common functional forms of salinity induced reductions in crop water uptake, rather than being tied to one particular representation; and (iv) the utilized modeling framework is compatible with leading transient-state numerical models.

1. Introduction

Maintaining the productivity of irrigated croplands in arid and semiarid regions requires water management practices that prevent excessive accumulation of harmful salts in the root zone. Standard guidelines for managing salinity and irrigation [*U.S. Salinity Laboratory Staff*, 1954; *Ayers and Westcot*, 1985] were mostly designed with the goal of maintaining root zone salinity at a level that avoids any reductions in crop growth or yield. Yet achieving maximum yield is frequently not optimal with respect to either grower profits or environmental conservation, particularly when water resources are limited [*Dinar et al.*, 1985; *Kan et al.*, 2002]. Since the availability of good quality water for irrigation is decreasing in many parts of the world [*Falkenmark and Rockström*, 2006; *Strzepek and Boehlert*, 2010], there is a growing need for management tools that can target submaximal yields and support the use of lower-quality (saline) irrigation waters.

Various models of irrigated systems provide a possible means for developing improved water management guidelines. Two general classes of models have been identified in the literature: transient-state and steady-state. Several authors have suggested that comprehensive, transient-state numerical models such as UNSATCHEM [*Suarez and Simunek*, 1997], HYDRUS [*Šimůnek et al.*, 2013], ENVIRO-GRO [*Pang and Letey*, 1998], and SWAP [*van Dam et al.*, 2008] represent the best opportunity going forward for designing and implementing improved irrigation management [*Letey and Feng*, 2007; *Ditthakit*, 2011; *Letey et al.*, 2011; *Oster et al.*, 2012]. Such models allow for consideration of site-specific soil, water, and crop parameters, and can account for time-varying field conditions. However, experimental data on the response of crops to time-varying stresses are relatively limited, and it is not yet clear that model representations are sufficient to justify their use in irrigation management [e.g., *Rhoades*, 1999; *Skaggs et al.*, 2014]. Furthermore, developing procedures for routine use of such highly parameterized, relatively complex models is challenging and ongoing [*Suarez*, 2012; *Skaggs et al.*, 2013, 2014].

Steady-state (time invariant) models use comparatively simple representations of soils and crops, and have relatively modest data requirements. True steady-state conditions do not exist in irrigated systems, but over

sufficiently long time periods (a season or more), steady-state may become a reasonable approximation, and indeed steady-state crop-water production models have shown reasonably good agreement with experimental data [*Letey et al.*, 1985; *Shani et al.*, 2007]. On the other hand, various studies have found that steady-state modeling analyses tend to recommend more irrigation and salt leaching than is necessary [*Hoffman*, 1985; *Letey*, 2007; *Letey and Feng*, 2007; *Corwin et al.*, 2007]. Most steady-state models and assessment equations assume it is possible to specify a priori a fixed value for either the crop evapotranspiration rate or the leaching fraction. This assumption is reasonable only if root zone salinity is not limiting crop water use, such that the actual evapotranspiration rate and the nonlimited rate are the same. When salinity limits water uptake, the actual evapotranspiration (or leaching fraction) cannot be specified a priori [*Suarez*, 2012].

Although literature discussions of steady-state and transient-state models have sometimes presented the two frameworks as an either-or proposition, both types of models have their place in water management and salinity assessments. For certain types of assessments, the level of detail provided by steady-state models is more appropriate than that given or required by transient-state models. In other assessments, a transient-state model may be preferred. In many cases, it would surely be beneficial to use both approaches concurrently, with a range or hierarchy of outputs from multiple models giving some indication of the precision or uncertainty in model predictions, and possibly providing insight into the impact of various model assumptions.

The objective of the present work was to develop a steady-state model that improves on existing models and that can easily be used in concert with transient-state models. In the literature, two approaches to steady-state modeling have been pursued. The first relies on a general physical-mathematical model of the root zone and water uptake processes [*Raats*, 1975, 1981; *Hoffman and van Genuchten*, 1983; *Bresler and Hoffman*, 1986]. The limitation of these analyses is that they assume or require that plant water uptake is not affected (reduced) by root zone salinity. Thus these models are mainly useful for identifying irrigation or leaching requirements that produce maximum crop yields. The second modeling approach [*Letey et al.*, 1985; *Shani et al.*, 2007] allows for consideration of submaximal crop yields and deficit irrigation rates, but instead of a general physical-mathematical framework, the approach relies on ad hoc formulations that may be difficult to reconcile with mechanistic transient-state models. Additionally, these ad hoc models require iterative solution techniques, limiting their ease of use.

Herein, we bridge the divide between the two steady-state approaches, presenting a general physical-mathematical model that can account for reduced water uptake due to root zone salinity. Two analytical solutions are derived, corresponding to two different functional forms of the uptake reduction function. The solutions are explicit (require no iterative techniques) and permit the direct calculation of the solute concentration profile, the water flux profile, the crop transpiration rate, and (using standard approximations) the crop yield. Example applications are illustrated, including the calculation of irrigation requirements for submaximal yields, and the generation of crop-water production functions for varying irrigation waters, irrigation rates, and crops. Comparisons with existing models and experimental data are presented.

2. Model Formulation

2.1. Mass Balance

Conservation of water and solute during steady-state, one-dimensional flow and transport can be written as

$$\frac{dq}{dz} + S_w(z) = 0 \tag{1a}$$

$$\frac{d(qC)}{dz} = 0 \tag{1b}$$

where q is the water flux density, C is the solute concentration, S_w is a sink term associated with root water uptake, and z is the vertical space coordinate, defined positive downward with the soil surface at $z = 0$. Equation (1) disregards solute sorption and dispersion, mineral precipitation and dissolution, and the uptake of solute by plants.

2.2. Root Water Uptake

The root water uptake sink term is defined

Table 1. Equations for Unstressed Water Uptake Profiles[a]

Model	$b(Z)$	$B(Z)$	$B^{-1}\ (p: 0 \le p < 1)$
40:30:20:10	$(9-8Z)/(5L)$	$(9Z-4Z^2)/5$	$(9-\sqrt{81-80p})/8$
Trapezoid	$\begin{cases} 5/(3L) & 0 \le Z \le 0.2 \\ (25-25Z)/(12L) & 0.2 < Z \le 1 \end{cases}$	$\begin{cases} 5Z/3 & 0 \le Z \le 0.2 \\ (50Z-25Z^2-1)/24 & 0.2 < Z \le 1 \end{cases}$	$\begin{cases} 3p/5 & p \le 1/3 \\ 1-\sqrt{(24/25)(1-p)} & p > 1/3 \end{cases}$
Exponential	$\exp(-ZL/\delta)/\delta$	$1-\exp(-ZL/\delta)$	$-(\delta/L)\ln(1-p)$

[a]Rooting depth is L; dimensionless depth is $Z=z/L$; $b \equiv 0$; and $B \equiv 1$ for $Z > 1$.

$$S_w(z,C) = T_p b(z) \alpha(C) \tag{2}$$

where $b(z)$ is the potential water uptake density profile, α is a reduction function specifying decreases in uptake that occur with increasing C, and T_p is the potential transpiration rate. The uptake density profile is normalized so that

$$\int_0^L b(z)\,dz = 1 \tag{3}$$

where L is the depth of the root zone. The actual transpiration rate is given by

$$T = \int_0^L S_w(z,C)\,dz = T_p \int_0^L b(z)\alpha(C)\,dz \tag{4}$$

The general form of equation (2), with transpiration being expressed as a macroscopic potential rate that may be diminished by the presence of depth-varying root zone stressors [*Feddes et al.*, 1978; *Skaggs et al.*, 2006], is common in transient-state numerical models of root zone processes (such as those mentioned above), but to our knowledge it has not been utilized in steady-state analyses of crop production with saline waters.

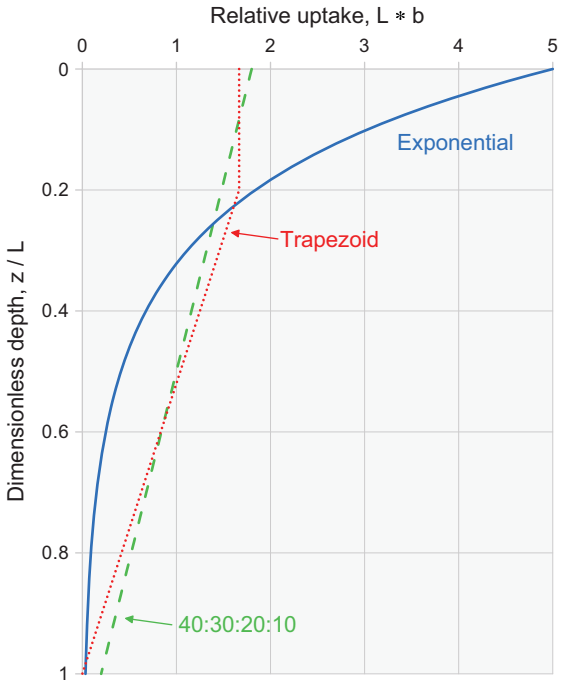

Figure 1. Illustration of the unstressed uptake profiles specified by the models listed in Table 1.

2.3. Unstressed Uptake Density Profiles

Following *Hoffman and van Genuchten* [1983], we consider from the literature several possible equations for the potential (unstressed) uptake density profile, $b(z)$ (Table 1 and Figure 1). The "40:30:20:10" model specifies a linearly decreasing uptake pattern such that 40% of the uptake is in the top quarter of the root zone, 30% is in the second quarter, and so on. A 40:30:20:10 pattern was assumed in many classical analyses of saline soils [*Rhoades*, 1999]. The trapezoid model specifies uniform uptake in the top 20% of the root zone, and a linear decrease with depth below that. The uptake ratio for the four quarters of the root zone is 41:33:20:6. The trapezoid model used here specifies that uptake occurs throughout the root zone (after M. Th. van Genuchten, A numerical model for water and solute movement in and below the root zone, unpublished research report, U.S. Salinity Lab., USDA, ARS, Riverside, Calif., 1987).

Table 2. Model Uptake Reduction Functions

Model	Parameters	$\alpha(C)$
Sigmoid	$C50$	$\left[1+(C/C50)^3\right]^{-1}$
Threshold	S, C_T	$\begin{cases} 1 & C \le C_T \\ 1-S(C-C_T) & C_T < C < C_T+1/S \\ 0 & C \ge C_T+1/S \end{cases}$

This is slightly different from the trapezoid model used by *Hoffman and van Genuchten* [1983], where uptake did not occur in the bottom 20%. The final model is the exponential model of *Raats* [1975], which contains a shape parameter δ (Table 1). In Figure 1 (and throughout this manuscript), δ was taken to be $\delta=L/5$ [after *Hoffman and van Genuchten*, 1983]. With this parameterization, a small error is introduced because the integral of $b(z)$ over the depth of the root zone is equal to 0.993 (rather than 1). The exponential model specifies a greater proportion of uptake near the surface (Figure 1), with an uptake ratio of 71:20:6:2.

2.4. Uptake Reduction Functions

Crop yield reductions in response to soil salinity are most often modeled with either a threshold-type function [*Maas and Hoffman*, 1977] or a sigmoid (S-shaped) function [*van Genuchten and Gupta*, 1993]. Models that use equation (2) (or equivalent) to simulate root water uptake under salinity stress generally assume the local reduction function α has the same functional form(s) [*Skaggs et al.*, 2006; van Genuchten, unpublished research report, 1987]. Thus, we consider two possibilities for α, a sigmoid function and a threshold model (Table 2 and Figure 2). In the sigmoid model, the crop-specific parameter $C50$ is the solute concentration at which root water uptake is reduced by half. We use an exponent of "3" in the sigmoid model, which is the approximate mean value found by *van Genuchten and Gupta* [1993] in their review and analysis of plant salt tolerance data. *van Genuchten and Gupta* [1993] found that the fit of the sigmoid model to relative yield data was not greatly affected regardless of whether the exponent was fixed at 3 or treated as a fitting parameter. A value of 3 has also been recommended for modeling local uptake within the root zone [*Šimůnek et al.*, 2013]. In the present work, fixing the exponent is convenient because plant salt tolerance is then quantified by a single parameter, $C50$.

The threshold model is patterned after the classic Maas-Hoffman yield reduction function [*Maas and Hoffman*, 1977]. The model stipulates that uptake occurs at potential rates where the concentration is below a crop-specific threshold value C_T. Above the threshold, uptake decreases linearly with increasing C. The slope parameter S specifies the fractional decrease in uptake per unit increase in concentration.

As discussed below, the parameters $C50$, C_T, and S can be estimated for specific crops based on tabulations of plant salt tolerance parameters.

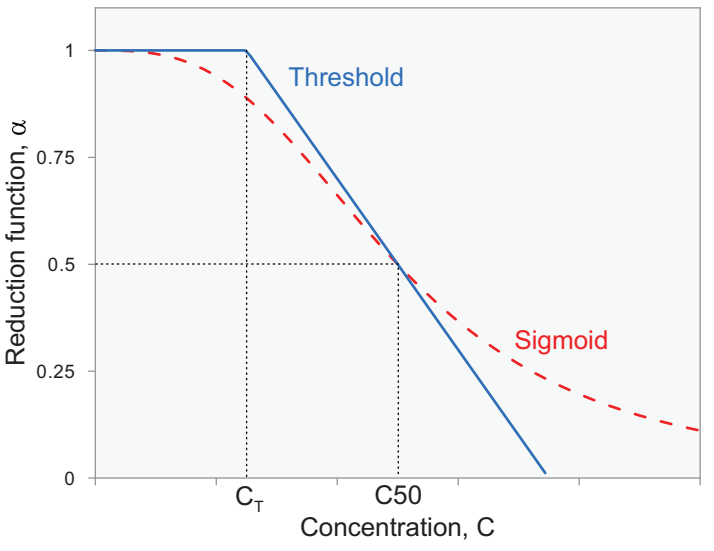

Figure 2. Illustration of the "threshold" and "sigmoid" uptake reduction functions.

2.5. Water Balance

At steady-state, water balance for an irrigated system can be expressed

$$D+E+T=I \qquad (5a)$$

where D is the drainage rate, E is the evaporation rate, T is the transpiration rate, and I is the irrigation rate. Where precipitation is not negligible, I may be taken to be equal to the sum of the irrigation and precipitation rates. Alternatively, equation (5a) may be written

$$D/I+E/I+T/I=1 \qquad (5b)$$

where the terms on the left-hand side are the drainage

Table 3. Analytical Solutions for Steady-State Concentration Profiles

Model Parameterization	C/C_0
Sigmoid reduction function, $C(Z; C_0, T_p, q_0, B, C50)$	$C(Z)/C_0 = \begin{cases} \left(R+\sqrt{\Delta}\right)^{1/3}+\left(R-\sqrt{\Delta}\right)^{1/3} & \Delta \geq 0 \\ 2\sqrt{-Q}\cos(\theta/3) & \Delta < 0 \end{cases}$
Threshold reduction function, $C(Z; C_0, T_p, q_0, B, C_T, S)$	$C(Z)/C_0 = \begin{cases} 1/J & Z \leq H^{-1}[(1-C_0/C_T)/(T_p/q_0)] \\ \dfrac{1+C_T S}{C_0 S[1+W_0(A)]} & \text{otherwise} \end{cases}$
Definitions	
$Z=z/L$	$J = 1-(T_p/q_0)B(Z)$ $\quad (\cdot)^{1/3}$ = real cube root
Sigmoid:	
$\Delta=Q^3+R^2$	$R = (C50/C_0)^3$ $\quad Q = (2JR-1)/3$ $\quad \theta = \cos^{-1}\left(R/\sqrt{-Q^3}\right)$
Threshold:	
$A=F\exp(G+F)$	$F = 1+C_T S/C_M S-1$ $\quad G = (1+C_T S)^2[J-C_0/C_M]/C_0 S$
$C_M=\max(C_0, C_T)$	$W_0(\cdot)$ = Lambert W function $\quad H^{-1}[a] = \begin{cases} 0 & a < 0 \\ \infty & a \geq 1 \\ B^{-1}(a) & \text{otherwise} \end{cases}$

fraction, evaporative fraction, and transpiration fraction, respectively. In the soil salinity literature, the drainage fraction is alternatively known as the leaching fraction.

3. Results

3.1. Analytical Solutions

The boundary conditions for equation (1) are:

$$q(z=0) \equiv q_0 = I-E \tag{6a}$$

$$C(z=0) \equiv C_0 = C_{IR}\frac{I}{I-E} \tag{6b}$$

where C_{IR} is the solute concentration of the irrigation water. If precipitation is a significant component of I, or if more than one irrigation water is used, then C_{IR} can be taken to be a weighted average of the concentrations [e.g., *Bradford and Letey*, 1992]. In the simplest case of zero evaporation ($E = 0$), the inlet water flux is equal to the irrigation rate, $q_0=I$, and the inlet concentration is equal to the irrigation water concentration, $C_0=C_{IR}$.

For both forms of $\alpha(C)$ considered in the present work, equation (1) can be solved analytically to obtain an explicit solution for $C(z)$. Table 3 gives the solutions for both reduction functions. The solutions are expressed in terms of an arbitrary cumulative uptake profile,

$$B(z) = \int_0^z b(z')\mathrm{d}z' \tag{7}$$

Specific equations for B are given in Table 1 for each of the three considered model uptake profiles. The threshold solution also requires the inverse of the cumulative uptake, B^{-1}. Equations for B^{-1} are given in Table 1.

The methods used to obtain the analytical solutions in Table 3 are outlined in Appendix A. The analytical solutions were verified by confirming that they matched results obtained when equations (1) and (6) were solved numerically in Mathematica 7 using default settings for the NDSolve function [*Wolfram Research*, 2008].

The water flux in the soil profile can be determined from the concentration profile,

$$q(z) = q_0 C_0 / C(z) \tag{8}$$

Equation (8) is obtained by integrating equation (1b) and applying equation (6). The actual transpiration rate can be calculated from equation (4), but it is more convenient to make the calculation based on the concentration at the bottom of the root zone,

$$T = q_0(1 - C_0/C_L) \tag{9}$$

where $C_L \equiv C(z=L)$. Equation (9) can be derived for our model from equations (5), (6), and (8), although it holds true more generally [e.g., *Hoffman and van Genuchten*, 1983]. Notice that C_L and hence the actual transpiration rate T are not affected by the functional form used for b. The reason is that the variation of C with depth depends entirely on the variation of $B(z)$, and, by definition, $B(z=L)=1$ for all uptake profiles (excepting the small error introduced in the case of the exponential model, as noted above).

3.2. Comments

The models predict a root zone solute concentration that increases monotonically with depth. When the threshold reduction function is used, the root zone may encompass three distinct water uptake regions depending on the irrigation rate, crop salt tolerance, and irrigation water concentration. If the inlet concentration is less than the threshold concentration ($C_0 < C_T$), then uptake in the upper part of the root zone occurs at potential or unstressed rates. The depth of this zone depends on the relative effective irrigation rate, q_0/T_p. Higher irrigation rates push the depth of the unstressed region further downward. If $q_0/T_p \geq (1-C_0/C_T)^{-1}$, the unstressed region spans the entire root zone. For irrigation rates smaller than that cutoff value, the concentration in the root zone will exceed the threshold concentration at $z/L = B^{-1}\left[(1-C_0/C_T)/(T_p/q_0)\right]$. Below that depth, uptake is reduced according to the linearly decreasing section of the reduction function. If the inlet water concentration is greater than the threshold concentration ($C_0 > C_T$), then an unstressed section of the root zone does not exist and uptake is reduced starting at the soil surface. A third region exists if the concentration in the root zone reaches $1/S+C_T$. At this maximum concentration, water uptake ceases, and the concentration in the soil from that point downward is $1/S+C_T$. Appendix A provides additional details regarding the delineation of the uptake regions and their seamless representation in the solution given in Table 3.

Uptake processes are comparatively simple when the sigmoid model is used. Uptake is reduced below potential rates throughout the root zone, although the reduction may be very minimal at low solute concentrations. Likewise, no maximum concentration exists at which uptake completely stops, although uptake may approach zero at high concentrations.

For all model formulations, drainage is always predicted to occur, even for deficit irrigation rates ($q_0/T_p < 1$). The reason is that in the long run (steady-state), salinity in the root zone will always increase to a point where the resultant reductions in uptake will be sufficient to generate drainage [e.g., *Dudley et al.*, 2008].

3.3. Dimensionless Parameter Groups

The model with the sigmoid reduction function depends on two dimensionless parameters groups: q_0/T_p and $C_0/C50$. With the threshold model, the solution depends on three groups: q_0/T_p, C_TS, and C_0S. The latter two terms can be combined as $C_0S/(1+C_TS)=C_0/(1/S+C_T)$. The maximum concentration $1/S+C_T$ is a reasonable single-value quantification of crop salt tolerance when the threshold model is used, so $C_0/(1/S+C_T)$ can be viewed as a measure of the irrigation water concentration relative to the crop salt tolerance. The same measure is provided by $C_0/C50$ in the sigmoid model.

3.4. Examples

Figure 3 shows concentration profiles calculated for a deficit irrigation scenario ($q_0/T_p=0.7$) using the threshold and sigmoid uptake reduction functions in combination with each of the three model uptake profiles, $b(z)$. We consider first the impact of the uptake profile. It is apparent from Figure 1 that the 40:30:20:10 and trapezoid models are very similar. It is therefore not surprising that, in Figure 3, concentration profiles computed with those two uptake models are also similar (for a given reduction function). The exponential uptake profile specifies a greater percentage of uptake in the top section the root zone, and consequently, with either reduction function, the predicted concentrations are higher near the surface and throughout

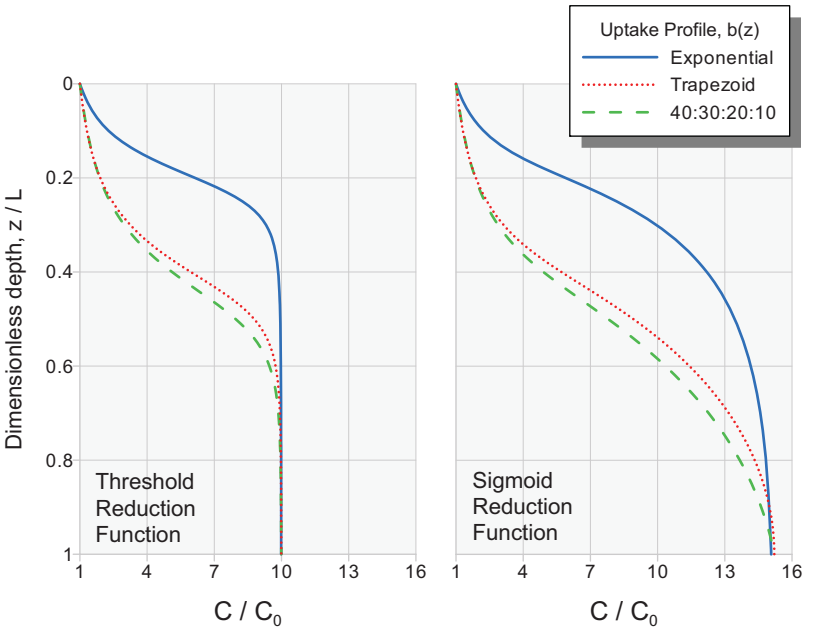

Figure 3. Concentration profiles predicted for the sigmoid or threshold uptake reduction functions in combination with either an exponential (solid), 40:30:20:10 (dashed), or trapezoid (dotted) uptake density profile. The plots were drawn with $q_0/T_p=0.7$, $C_0/(1/S+C_T)=0.1$, $C_TS=0.3$, and $C_0/C50=C_0S/(0.5+C_TS)$.

most of the root zone. However, as was noted above, the concentration at the bottom of the root zone (the drainage concentration) is the same regardless of the model used for $b(z)$.

We next consider the impact of the uptake reduction function, $\alpha(C)$ (Figure 3). In the upper part of the root zone where salinity is relatively low, the concentration profiles computed with the two reduction functions are very similar, but deeper in the root zone the profiles diverge significantly because the threshold model specifies that uptake ceases when the concentration reaches $1/S+C_T$ (Figure 2). Recall that the higher drainage concentration predicted in this case using the sigmoid model corresponds also to a higher predicted actual transpiration rate.

The differences depicted in Figure 3 between the solute profiles (and actual transpiration rates) obtained for the two reduction functions depend on the irrigation rate and irrigation water salinity. Figure 4 shows concentration profiles computed for each reduction function with three irrigation rates, q_0/T_p, and two relative irrigation water salinities, $C_0/(1/S+C_T)$. The plots in Figure 4d correspond to the scenario depicted in Figure 3. The exponential uptake profile was used for all calculations in Figure 4. Figures 4c and 4f also show concentration profiles calculated with equation (A9), which is the solution when there is no uptake reduction ($\alpha=1$) and uptake occurs at potential rates. That solution exists only for $q_0/T_p > 1$. For the nondeficit ($q_0/T_p \geq 1$) irrigation cases in Figures 4b, 4c, 4e, and 4f, the concentration profiles are only minimally impacted by the choice of uptake reduction function. Slightly higher drainage concentrations are predicted using the threshold model (Figures 4b, 4c, 4e, and 4f) because the threshold function specifies a higher rate of uptake under low to moderate salinity stress conditions (Figure 2).

Although the trends depicted in Figure 4 hold generally, some details depend on the specific parameter values. Besides the irrigation rates and inlet concentration values indicated on the figure, the threshold plots in Figure 4 were all drawn with $C_TS=0.3$. As a point of reference, salt tolerance data reported by *Maas and Hoffman* [1977] suggest that for forages, fruits, and vegetables C_TS ranges approximately from 0.05 to 0.6. The sigmoid plots were calculated with the salt tolerance parameter specified as $C_0/C50=C_0S/(0.5+C_TS)$, such that in each case the concentration at which 50% reduction occurred was the same for both uptake reduction models (as depicted in Figure 2). Although matching the two functions at 50% uptake reduction is convenient, it is not necessarily optimal in terms of minimizing the difference between the two functions [e.g., *Steppuhn et al.*, 2005].

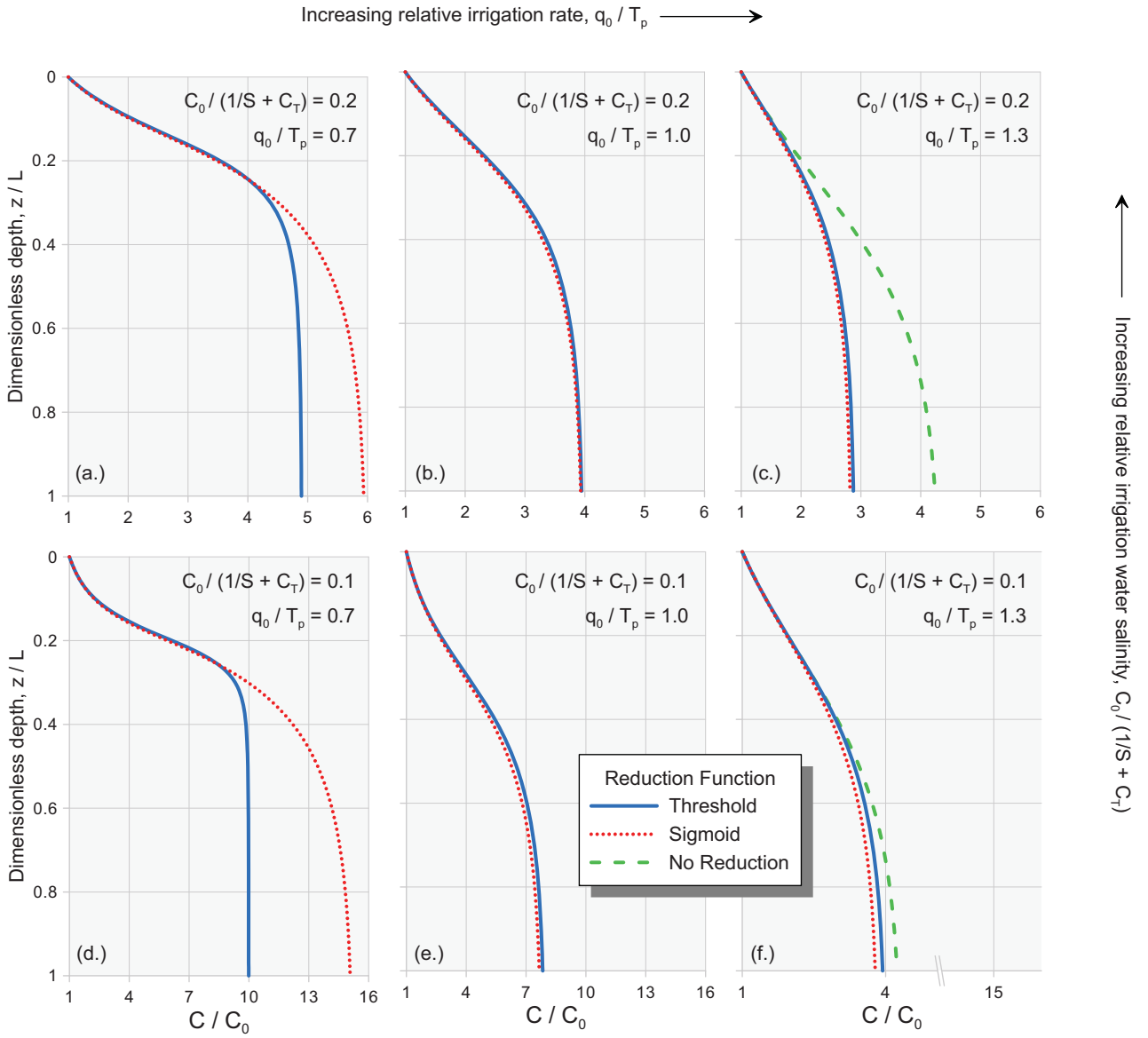

Figure 4. Concentration profiles predicted for various relative effective irrigation rates, q_0/T_p, and relative irrigation water salinities, $C_0/(1/S+C_T)$. The profiles in each plot were calculated using either the threshold (blue, solid) or sigmoid (red, dotted) uptake reduction function in combination with the exponential uptake density profile. (c and f) For cases where $q_0/T_p > 1$, concentration profiles calculated assuming no reductions in uptake due to salinity are also shown (green, dashed). The other model parameters were specified as $C_TS=0.3$ and $C_0/C50=C_0S/(0.5+C_TS)$.

4. Discussion

4.1. Practical Considerations

For practical water management applications, it will be necessary or convenient to utilize several common approximations. The primary intended application of the presented models is assessments of crop production systems. For many crops, yield is proportional to transpiration, and it is common in modeling studies to define relative yield as

$$Y_R = Y/Y_p = T/T_p \tag{10}$$

where Y_R is the relative yield, Y is the crop yield, and Y_p is the maximum yield obtainable with a well-watered, unstressed crop. Thus, Y_R can be calculated with equation (9).

Because water and soil salinities in agriculture are most often reported in terms of solution electrical conductivity (*EC*) rather than solute concentration, it is convenient to use the approximation that *EC* is

proportional to solution concentration. While not strictly correct, the approximation is sufficiently accurate for many irrigation management applications, and allows, for example, the substitution $C_0/C50 = EC_0/EC50$.

Data for the salt tolerances of specific crops are mostly available in the form of tabulations of Maas-Hoffman slope (MH_S) and threshold (MH_T) coefficients that specify expected yield reductions as a function of soil salinity, where soil salinity is quantified in terms of the electrical conductivity of the soil saturation-paste extract, or EC_e. To use these salt tolerance coefficients in modeling studies having mechanistic descriptions of root zone processes, it is necessary to express the coefficients in terms of soil solution EC, rather than EC_e. Since Maas-Hoffman coefficients are typically estimated from controlled salt tolerance trials in which the root zone water content is maintained near-field capacity, i.e., at roughly half the saturation-paste water content, it is usually estimated that the reported EC_e is half the operative soil solution EC. With this approximation, parameters for the threshold reductions function, for example, can be estimated as

$$C_T = k \cdot 2MH_T \tag{11}$$

$$S = MH_S/2/k/100 \tag{12}$$

where k is the proportionality constant relating C and EC, and the numerical factor 100 accounts for the practice of Maas-Hoffmann coefficients being reported in terms of percentage yield reductions. The sigmoid reduction function parameter can be estimated from the threshold model parameters, $C50 = 0.5/S + C_T$, or it can be obtained from the tabulation of fitted values given by *van Genuchten and Gupta* [1993]. Due to the form of the dimensionless parameter groups discussed above, the parameter k drops out of the sigmoid or threshold model when calculating C/C_0 or Y_R, such that the results do not depend on the numerical value of k.

4.2. Applications and Comparisons With Other Models

4.2.1. Leaching Requirement

Traditional guidelines for managing salinity in irrigated agriculture have emphasized the leaching fraction (LF), which, as we noted previously, is also called the drainage fraction (D/I). Solute mass balance considerations show that

$$\mathrm{LF} = D/I = C_{IR}/C_L \approx EC_{IR}/EC_L \tag{13}$$

The leaching requirement (LR) is defined as the minimum LF that is required to maintain the root zone salinity at a level that does not reduce yields below acceptable levels. The LR may be expressed

$$\mathrm{LR} = EC_{IR}/EC_L^* \tag{14}$$

where EC_L^* is given an asterisk to indicate that it is the target salinity level that must be maintained at the bottom of the root zone to maintain yields for a given crop. Using an LR that is larger than necessary leads to wasteful overirrigation and groundwater degradation. An important issue in classical soil salinity literature was the specification of an appropriate value for EC_L^*. *Hoffman* [1985] gives an overview of various formulations that were used.

The meaning of "acceptable" reductions in the above definition is open to interpretation, but most LR analyses have targeted relative yields of 100%. The sigmoid version of the model developed herein is not strictly compatible with a goal of 100% relative yield. The predicted yield may approach 100%, but it cannot be reached. The threshold version predicts 100% yield if the entire root zone is maintained below the threshold concentration, i.e., if $q_0/T_p \geq (1 - C_0/C_T)^{-1}$. This condition is equivalent to specifying equation (14) with $EC_L^* = 2MH_T$. The resulting LR is larger than historical recommendations, and judging from data reviewed by *Hoffman* [1985], is generally larger than necessary to obtain 100% yield. Other model-based leaching recommendations have also been found to be excessively large, and *Hoffman* [1985] has suggested that a correction to model-based predictions of the leaching requirement, such as that implemented by *Hoffman and van Genuchten* [1983], be used to bring the recommendations in line with available experimental data. The reason for the discrepancy between experimentally determined and model estimated LRs is not known, but a contributing factor may be that it is difficult to determine experimentally an exact LF at which 100% yield is obtained. It has long been known that the relationship between soil salinity and irrigation rate flattens out near maximum yield [e.g., *Bower et al*., 1969]. Consequently, it may be difficult to distinguish experimentally, say, 97 and 100% yield, whereas a model calculation will seek 100% yield even though, in that flat part

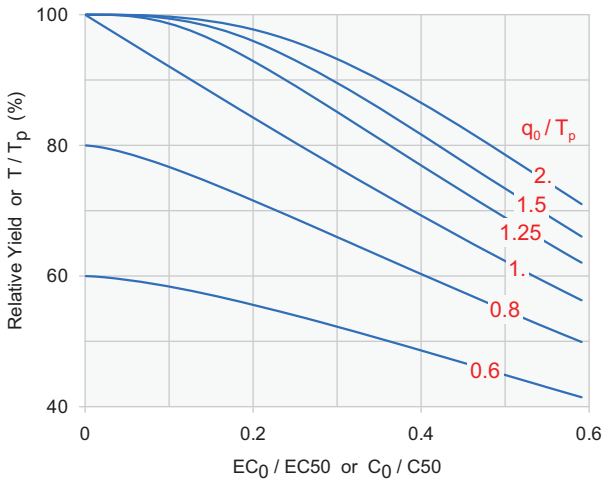

Figure 5. General relationship between crop yield, effective irrigation water salinity (EC_0 or C_0), crop salt tolerance ($EC50$ or $C50$), and irrigation rate (q_0/T_p) as calculated with the sigmoid analytical solution.

of the curve, a substantial increase in irrigation may be required to go from 97 to 100%. Also, in many experiments, crop growth may be affected by factors other than salinity when salinity is low and yields are near 100%, such that the relationship between leaching/irrigation rate, soil salinity, and crop yield may be obscured.

Of greater interest to the current work are model calculations for lower irrigation rates and submaximal yields, a situation for which the results are in better agreement with experimental data (shown below). A simple relation between LF and irrigation rate exists only in the case of 100% yield. In the models developed above, the LF is not specified. Rather, the LF is an outcome that results from the specification of the irrigation rate, irrigation water salinity, and crop salt tolerance. Thus, it is more useful to think in terms of an irrigation requirement rather than a leaching requirement. An example is given in Figure 5, which shows the general relationship between irrigation water salinity, crop salt tolerance, irrigation rate, and relative yield as predicted with the sigmoid analytical solution. For a given water (EC_0) and crop ($EC50$) combination, the irrigation requirement for a particular yield is found by locating $EC_0/EC50$ along the x axis and going up from there to find the irrigation rate that intersects with the target yield. Notice the diminishing returns that are obtained from increasing irrigation as yield approaches 100%. A similar diagram can be made for the threshold model, although because of the extra parameter group, the diagram consists of multiple contour plots of yield, one for each value of q_0/T_p, with the two independent variables of each plot being C_TS and C_0S (not shown).

Figure 5 is comparable to the leaching fraction diagrams found in standard soil salinity texts [e.g., *Hoffman and van Genuchten*, 1983; *Rhoades*, 1999]. An alternative way to view the information in Figure 5 is to plot yield as a function of irrigation rate, with the resulting plot being termed the crop-water production function [*Letey et al*., 1985]. This is the perspective that has been favored in steady-state modeling analyses targeting submaximal yields. We consider those analyses in detail in the remainder of this paper.

4.2.2. Shani et al. [2007]

Shani et al. [2007, 2009] proposed that under steady-state conditions, crop transpiration can be modeled with the following expression,

$$T=\frac{\min\left\{T_p,\left[\left(\frac{{K_s}^{1/\eta}\psi_w}{(q_0-T)^{1/\eta}}-\psi_{root}\right)(q_0-T)\beta\right]\right\}}{1+\left\{\frac{q_0 EC_{IR}\left[\theta_r+(\theta_s-\theta_r)\left(\frac{q_0-T}{K_s}\right)^{1/\delta}\right]}{EC_e50\cdot(q_0-T)\theta_s}\right\}^3} \tag{15}$$

where K_s, η, δ, θ_s, θ_r, and ψ_w are (Brooks-Corey) soil hydraulic parameters, ψ_{root} is a pressure head associated with the root system, β is a resistance coefficient associated with water transfer between soil and root, EC_{IR} is the electrical conductivity of the irrigation water, and EC_e50 is the salinity at which crop yield is reduced by 50%, expressed on a saturation-paste extract basis. See *Shani et al*. [2007] for full details. The model has been used in several analyses [e.g., *Ben-Gal et al*., 2008; *Kan and Rapaport-Rom*, 2012; *Ben-Gal et al*., 2013].

Equation (15) is an implicit formula for T that must be solved iteratively. The denominator on the right-hand side accounts for salinity related reductions in transpiration; it is based on the whole-plant response function of *van Genuchten and Gupta* [1993]. The numerator accounts for water stress reductions. Below a certain level of soil wetness, uptake is reduced according to the Hanks model. Above that level, water stress reductions do not occur and the numerator evaluates to T_p. *Shani et al*. [2007] found that calculations made with equation (15) were mostly insensitive to the ψ_{root} parameter that appears in the numerator via the

Hanks model. The reported insensitivity is consistent with the observation made above that at steady-state, salinity stresses dominate water stresses even at low irrigation rates. For most parameter combinations and irrigation rates of interest, we find that the numerator evaluates to T_p.

4.2.3. Letey et al. [1985]

Letey et al. [1985] developed a crop-water production function for use with saline irrigation waters, which has been used subsequently in various economic and agronomic assessments [e.g., *Dinar et al*., 1985; *Vinten et al*., 1991; *Schwabe et al*., 2006]. In *Letey et al*. [1985] model, crop yield Y is estimated to be

$$Y = Y_{NS} - Y_D \tag{16}$$

where Y_{NS} is the yield that would be obtained in the absence of salinity stress and Y_D is the yield decrement that occurs due to salinity. Yield in the absence of salinity is assumed to be a function of the irrigation rate as follows:

$$Y_{NS} = \begin{cases} \frac{q_0}{T_p} Y_p & q_0 < T_p \\ Y_p & q_0 \geq T_p \end{cases} \tag{17}$$

The yield decrement is defined implicitly by one of the following two expressions, depending on the irrigation rate. For $q_0 < T_p$, Y_D is defined by

$$\frac{100}{EC_{IR} MH_S} \cdot \frac{Y_D T_p}{Y_p q_0} + \frac{MH_T}{EC_{IR}} = \frac{0.5 + 0.1 \ln\left\{\exp(-5) + Y_D T_p/(Y_p q_0)[1 - \exp(-5)]\right\}}{Y_D T_p/(Y_p q_0)} \tag{18a}$$

For $q_0 \geq T_p$, it is

$$\frac{100}{EC_{IR} MH_S} \cdot \frac{Y_D}{Y_p} + \frac{MH_T}{EC_{IR}} = \frac{0.5 + 0.1 \ln\left\{1 - \left[T_p/q_0 - Y_D T_p/(Y_p q_0)\right][1 - \exp(-5)]\right\}}{1 - T_p/q_0 + Y_D T_p/(Y_p q_0)} \tag{18b}$$

Equation (18) must be solved iteratively to determine Y_D.

The *Letey et al*. [1985] model is derived from consideration of the steady-state Maas-Hoffman crop response function and a steady-state calculation of average root zone salinity given by *Hoffman and van Genuchten* [1983]. To facilitate model comparisons, and to avoid introducing additional notation, we have in equations (16)–(18) imposed our terminology on the *Letey et al*. [1985] formulation. For example, the "maximum evapotranspiration" of *Letey et al*. [1985] has been equated with T_p, and "seasonal applied water" has been replaced with the effective irrigation rate, q_0. *Letey et al*. [1985] also proposed that, when considering a single growing season, a steady-state analysis could be extended by supposing that the growing season consists of two parts: an early season "transient" stage in which no drainage occurs, followed immediately by a steady-state stage. The result of such a modification is that an additional threshold parameter appears in equations (17) and (18). For our purposes, we have assumed that threshold is zero, which is consistent with a fully steady-state analysis. See *Letey et al*. [1985] for full details.

4.2.4. Model Comparisons

Figures 6 and 7 show predictions made for producing corn and sunflower, respectively, using the *Letey et al*. [1985] model, the *Shani et al*. [2007] model (Arava soil), and the two models developed herein. Also shown are experimental data presented by *Shani et al*. [2007]. The sigmoid and *Shani et al*. [2007] models were implemented using parameter values given by *Shani et al*. [2007] and the approximation that $EC50 = 2 \cdot EC_e50$, whereas the parameterization of the threshold and *Letey et al*. [1985] models were based on the salt tolerances given by *Maas and Hoffman* [1977]. The model predictions are generally all in agreement with one another, and also in agreement with the experimental data.

The obvious difference between the *Shani et al*. [2007] formulation and the other presented models is that equation (15) attempts to account for the effects of soil hydraulic properties. However, given that water flow and soil salinity are assumed to be at steady-state, it is not clear how or why soil properties should enter into the analysis. In the absence of water stress reductions in uptake, standard water flow and solute transport theory indicates that root zone concentrations at steady-state are not dependent on hydraulic properties (soil type). If water stress is present, reductions in uptake may occur that are dependent on soil type, but as noted, water stress is not expected to be significant at steady-state.

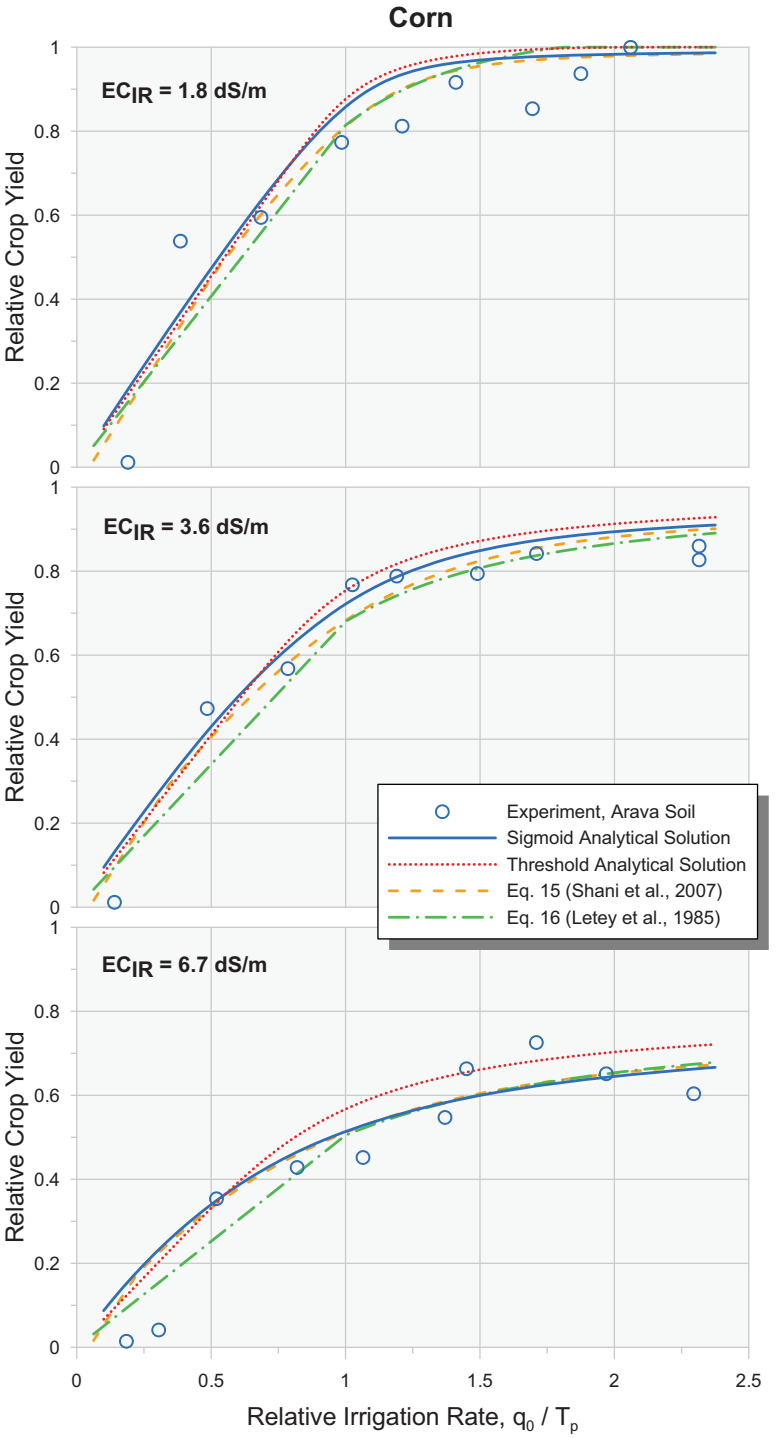

Figure 6. Comparison of model predicted crop-water production functions with experimental data for corn. Experimental data are from *Shani et al.* [2007].

This can be illustrated by considering the following example. As shown in Figures 6 and 7, calculations made with equation (15) using Arava soil parameters are in good agreement with model calculations made with the other (soil independent) models. Figure 8 presents another Arava soil example, comparing melon and pepper yield data with equation (15) and the sigmoid model. Model parameters and experimental data

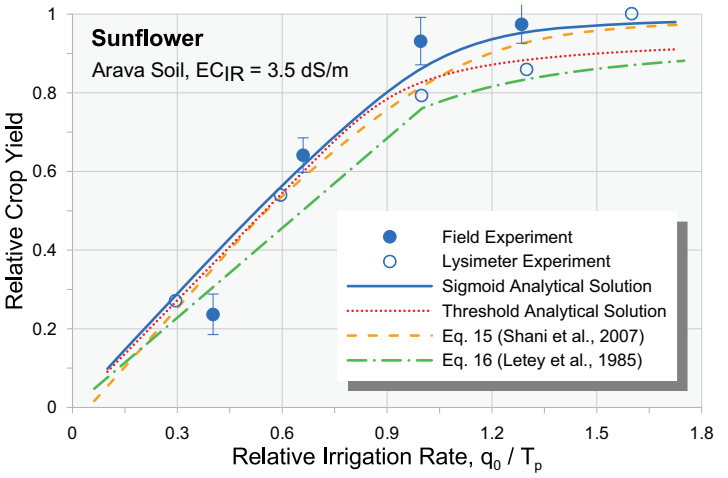

Figure 7. Comparison of experimental data with model predicted crop-water production functions for sunflower. Experimental data are from *Shani et al.* [2007].

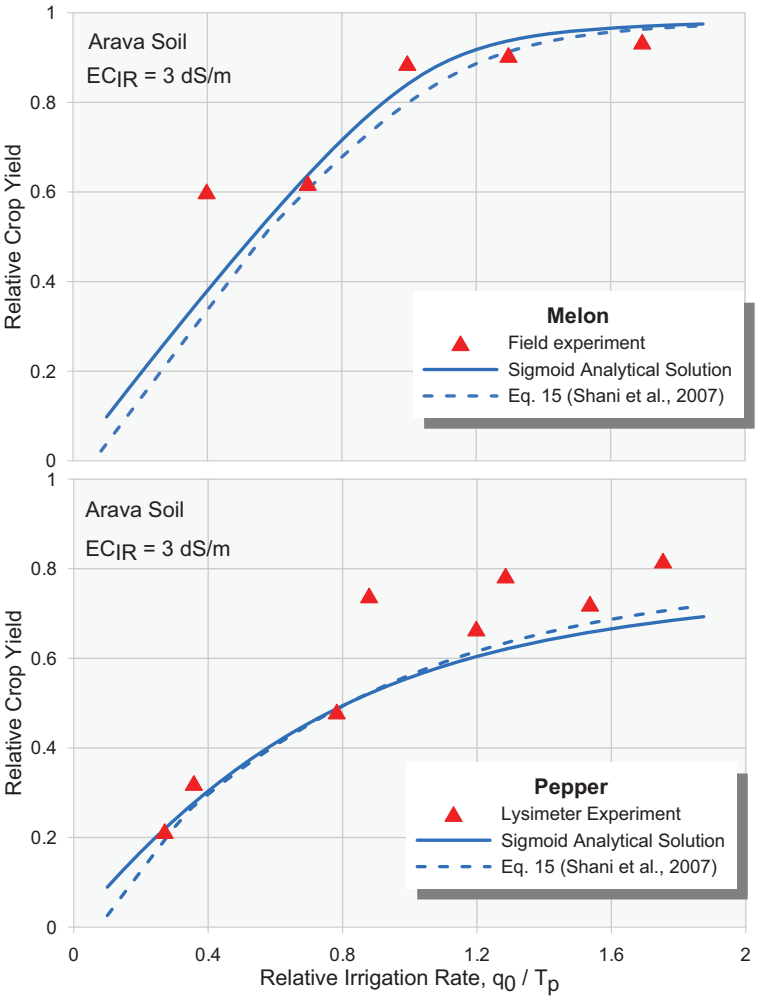

Figure 8. Comparison of experimental data with model predicted crop-water production functions for melon and pepper. Experimental data are from *Shani et al.* [2007].

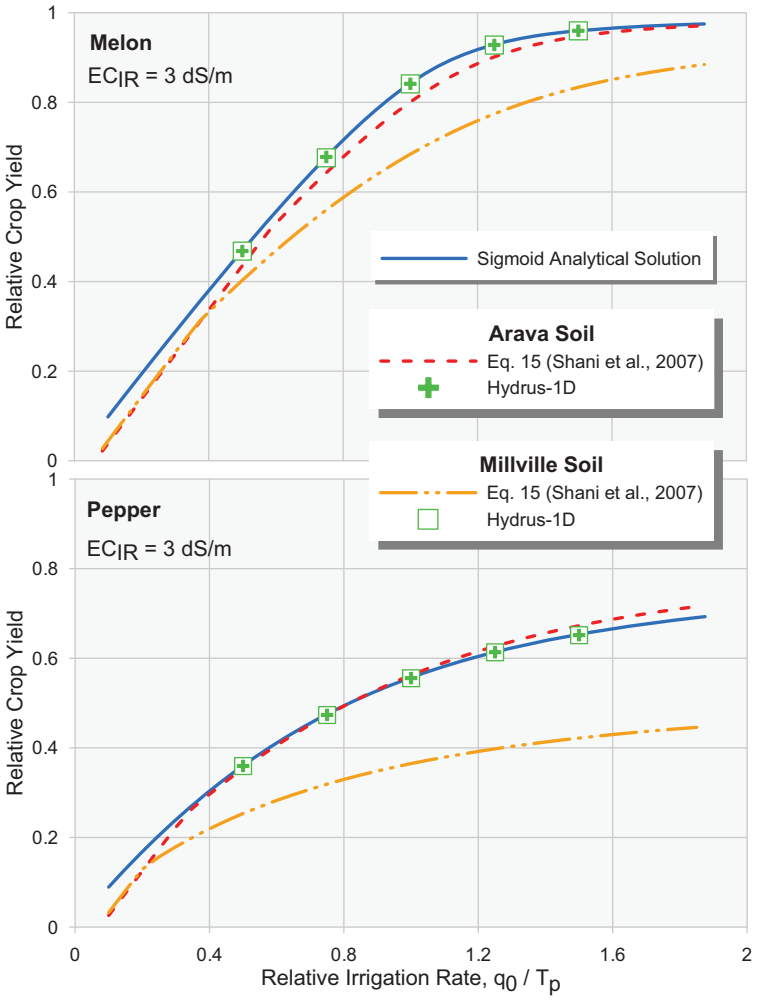

Figure 9. Comparison of melon and pepper yield predictions made with the sigmoid analytical solution, equation (15), and HYDRUS-1D for the Arava and Millville soils. The plots illustrate that the HYDRUS-1D predictions are (i) not affected by soil type and (ii) in very close agreement with the sigmoid analytical solution.

were taken from *Shani et al*. [2007]. Again, the model calculations are in good agreement with one another when equation (15) uses the Arava soil properties.

Figure 9 shows the same model calculations as Figure 8, along with calculations made with equation (15) for the Millville soil (parameters given by *Shani et al*. [2007]). Clearly, the agreement is poorer between the sigmoid analytical solution and the model calculation made for the Millville soil. Also shown in Figure 9 are calculations made with HYDRUS-1D [*Šimůnek et al*., 2013] for the two crops and soil types, accounting for both salinity and water stresses, and for differences in soil properties. As expected, the steady-state yields calculated with HYDRUS-1D were not affected by soil type or water stress, and were in close agreement with yield predictions made with the sigmoid analytical solution (Figure 9).

In reality, crop response to salinity is affected by a number of factors besides root zone solute concentrations, such as climate, solute composition, soil fertility, and cultural practices. It is also the case that prescribed irrigation rates may not be obtainable in a given soil due to, e.g., low hydraulic conductivity. Thus, more generally, crop-water production functions may vary with soil type. However, mechanisms associated with such factors are not present in the theory developed herein, nor do they exist in the reasoning presented in the formulation of equation (15). The primary dependence on soil type occurs in equation (15) because of an error: rather than calculate crop response to salinity based on soil solution concentrations and salt tolerance parameters which have been converted to a soil solution basis (as discussed above in regards the use of Maas-Hoffman coefficients), the reverse is done, with soil solution concentrations being

converted to an EC_e basis (actually, the conversion is to a saturated water content basis rather than a saturation paste basis, but these two water contents are apparently assumed to be approximately equal). This texture-dependent conversion of soil solution concentrations to some other fixed basis is incorrect in this context because, for example, identical salt concentrations (osmotic potentials) in, say, a loam and a sand would be converted differently and thus wrongly predicted to have differing effects on crop growth.

5. Conclusions

Due to the diminishing availability of good quality water for irrigation, it is increasingly important that irrigation and salinity management tools be able to target submaximal crop yields and support the use of marginal quality waters. Although steady-state models have limitations, they remain the best available option for many types of irrigation management and salinity assessments. Even when transient-state models are preferred, a consistently formulated steady-state analysis that considers the feedback of root zone salinity on water uptake can provide a useful baseline against which transient-state model predictions can be judged and evaluated.

Two explicit analytical solutions were developed in this work for steady-state analyses of crop production systems using marginal quality waters. Deficit irrigation rates and submaximal yields are supported. Predictions made with the new models are mostly consistent with comparable models from the literature, and have similarly reasonable agreement with experimental data. However, our solutions possess several advantages over existing models, including: (i) the solutions were derived from a complete physical-mathematical description of the system, rather than based on an ad hoc formulation; (ii) the analytical solutions are explicit and can be evaluated without iterative techniques; (iii) the solutions permit consideration of two common functional forms of salinity induced reductions in crop water uptake, rather than being tied to one particular representation; and (iv) the utilized modeling framework is consistent with leading transient-state numerical models.

Appendix A

This appendix outlines the procedures used to derive the analytical solutions for the solute concentration profile presented in Table 3. With boundary conditions given by equation (6), equation (1b) can be integrated to obtain equation (8) (i.e., $q=q_0C_0/C$). Substituting equation (8) into equation (1a) leads to

$$-q_0C_0\frac{\mathrm{d}(1/C)}{\mathrm{d}z}=\frac{q_0C_0}{C^2}\frac{\mathrm{d}C}{\mathrm{d}z}=T_p\alpha(C)b(z) \tag{A1}$$

Equation (A1) is an ordinary differential equation that can be separated and integrated,

$$\int_{C_0}^{C}\frac{\mathrm{d}C'}{C'^2\alpha[C']}=\frac{T_p}{q_0C_0}\int_0^z b(z')\mathrm{d}z'=\frac{T_p}{q_0C_0}B(z) \tag{A2}$$

Evaluation of the left-hand side depends on the model used for uptake reduction.

A1. Sigmoid Reduction Function

In the case of the sigmoid function (Table 2), the integral on the left-hand side of equation (A2) evaluates to

$$\int_{C_0}^{C}\frac{1+(C'/C50)^3}{C'^2}\mathrm{d}C'=\frac{1}{C_0}-\frac{1}{C}+\frac{C^2}{2(C50)^3}-\frac{(C_0)^2}{2(C50)^3} \tag{A3}$$

Combining equations (A2) and (A3) leads to a cubic equation for the concentration C which can be written as

$$\left(\frac{C}{C_0}\right)^3+3Q\frac{C}{C_0}=2R \tag{A4}$$

where Q and R are defined in Table 3. The values of coefficients Q and R are fixed by the values of model parameters: C_0, $C50$, T_p, q_0, and $B(Z)$. Cubic equations in the form of equation (A4) have three roots with properties (e.g., real or complex) and formulas that depend on the sign of the "polynomial discriminant," Δ

$=Q^3+R^2$ [*Weisstein*, 2014]. The formulas given for $C(Z)$ on the "$\Delta \geq 0$" and "$\Delta < 0$" branches of the solution in Table 3 correspond to the real, positive root of equation (A4) for those two conditions.

A2. Threshold Reduction Function

With the threshold function, the relative magnitude of the inlet (C_0) and threshold (C_T) concentrations must be considered. When $C_0 < C_T$, uptake in the top section of the profile occurs at the potential (unstressed) rate. At depths where concentration exceeds C_T, uptake is reduced according to the linearly decreasing section of the threshold reduction function. In the case of $C_T > C_0$, the concentration threshold is exceeded everywhere, and uptake reduction occurs throughout the root zone. For the stressed portion of the profile, we can accommodate both of these scenarios by writing the left-hand side of equation (A2) as

$$\int_{C_0}^{C} \frac{dC'}{C'^2 \alpha[C']} = \int_{C_0}^{C_M} \frac{dC'}{C'^2} + \int_{C_M}^{C} \frac{dC'}{C'^2 [1-S(C'-C_T)]} \tag{A5}$$

where C_M is the larger of (C_0, C_T). When $C_0 < C_T$ (and thus $C_M=C_T$), the first term on the right-hand side of equation (A5) corresponds to the unstressed section of the root zone, and the second to the stressed portion. For $C_0 > C_T$ ($C_M=C_0$), the first term vanishes and the second represents the whole profile. The integrals in equation (A5) can be evaluated analytically. Inserting the results into equation (A2) and performing some algebraic manipulations leads to:

$$\left(\frac{1+C_T S}{CS} - 1\right) \exp\left(\frac{1+C_T S}{CS} - 1\right) = F \exp(G+F) \tag{A6}$$

where F and G are defined in Table 3. Equations of this form satisfy [*Corless et al.*, 1996]

$$\frac{1+C_T S}{CS} - 1 = W_0[F \exp(G+F)] \tag{A7}$$

where $W_0[\cdot]$ is the principal branch of the Lambert W function. Solving equation (A7) for C gives the concentration in the stressed portion of the root zone,

$$C(Z) = \frac{1/S + C_T}{1 + W_0[F \exp(G+F)]} \tag{A8}$$

For $C_0 \geq C_T$, equation (A8) is the full solution. For $C_0 < C_T$, an equation for the unstressed section of the root zone is obtained by solving equation (1) with $\alpha=1$ [*Skaggs et al.*, 2007],

$$C(Z) = \frac{C_0}{1-(T_p/q_0)B(Z)} \tag{A9}$$

The transition from equation (A9) to (A8) occurs at the depth where $C=C_T$. From equation (A9), that depth is

$$Z = B^{-1}\left[(1-C_0/C_T)/(T_p/q_0)\right] \tag{A10}$$

where $B^{-1}[\cdot]$ is the inverse of the unstressed cumulative uptake profile (Table 1). Equations (A8) and (A9) are the two branches of the threshold solution in Table 3.

A special case exists if $C_0 < C_T$ and the irrigation rate is sufficiently high to keep the concentration below C_T throughout the root zone. This condition exists when the effective irrigation rate satisfies

$$q_0/T_p \geq (1-C_0/C_T)^{-1} \tag{A11}$$

The solution in this case is equation (A9). This case needs special attention only because it should be considered before attempting to evaluate equation (A10). The inverse function B^{-1} is defined only for arguments between 0 and 1, and if condition (A11) is satisfied, the argument of B^{-1} in equation (A10) would be invalid (≥ 1). We also note that, although not a problem for commonly encountered uptake profiles (Table 1), it is not guaranteed that B^{-1} exists for all uptake profiles (that is, no one-to-one mapping may exist between the cumulative uptake fraction and depth).

In summary, three possibilities exist when using the threshold model: (i) $C_0 \geq C_T$; (ii) $C_0 < C_T$ and $q_0/T_p \geq (1-C_0/C_T)^{-1}$; and (iii) $C_0 < C_T$ and $q_0/T_p < (1-C_0/C_T)^{-1}$. In Table 3, it was convenient to define a function H^{-1} that effectively extends the domain of B^{-1} and allows for a seamless handling of the three cases. The argument of H^{-1} is the same as that of B^{-1}, $a=(1-C_0/C_T)/(T_p/q_0)$. It can be verified that per the definition of H^{-1} in Table 3, $a \leq 0$ corresponds to case (i), $a \geq 1$ to case (ii), and $0 < a < 1$ to case (iii).

Lastly, the threshold model solution given in Table 3 assumes $C_0 < 1/S+C_T$. If this condition is not satisfied, the inlet concentration is so high that no water uptake occurs anywhere in the profile, and therefore $C(Z)=C_0$.

Notation

$b(z)$	normalized water uptake density profile (m^{-1}).
$B(z)$	cumulative water uptake profile.
C	solute concentration (kg m^{-3}).
C_0	effective inlet solute concentration (kg m^{-3}).
C_{IR}	irrigation water solute concentration (kg m^{-3}).
C_L	solute concentration at bottom of root zone (kg m^{-3}).
C_T	threshold concentration parameter (kg m^{-3}).
$C50$	half-yield concentration parameter (kg m^{-3}).
D	drainage rate (m s^{-1}).
E	evaporation rate (m s^{-1}).
EC	solution electrical conductivity (dS m^{-1}).
EC_e	saturation-paste extract electrical conductivity (dS m^{-1}).
EC_{IR}	irrigation water electrical conductivity (dS m^{-1}).
EC_L	soil solution electrical conductivity at bottom of root zone (dS m^{-1}).
$EC50$	half-yield soil solution electrical conductivity (dS m^{-1}).
I	irrigation rate (m s^{-1}).
L	depth of root zone (m).
LF	leaching fraction.
LR	leaching requirement.
MH_S	Maas-Hoffman slope parameter (% m dS^{-1}).
MH_T	Maas-Hoffman threshold parameter (dS m^{-1}).
q	water flux density (m s^{-1}).
q_0	effective inlet water flux (m s^{-1}).
S	slope parameter in threshold reduction function (m^3 kg^{-1}).
S_w	sink term for root water uptake (s^{-1}).
T	transpiration rate (m s^{-1}).
T_p	potential transpiration rate (m s^{-1}).
Y	crop yield (kg m^{-2}).
Y_p	potential yield, obtainable in the absence of all stresses (kg m^{-2}).
Y_{NS}	yield obtainable in the absence of salinity stress (kg m^{-2}).
Y_D	yield decrement due to salinity stress (kg m^{-2}).
z	vertical space coordinate (m).
Z	dimensionless depth ($=z/L$).
α	uptake reduction function.

Acknowledgment
The computer program scripts and data used in this manuscript can be accessed by contacting the corresponding author directly.

References

Ayers, R. S., and D. W. Westcot (1985), Water quality for agriculture, *FAO Irrig. and Drain. Pap. 29, Rev. 1*, Food and Agric. Org. of the U. N., Rome.

Ben-Gal, A., E. Ityel, L. Dudley, S. Cohen, U. Yermiyahu, E. Presnov, L. Zigmond, and U. Shani (2008), Effect of irrigation water salinity on transpiration and on leaching requirements: A case study for bell peppers, *Agric. Water Manage.*, *95*(5), 587–597, doi:10.1016/j.agwat.2007.12.008.

Ben-Gal, A., H.-P. Weikard, S. H. H. Shah, and S. E. A. T. M. van der Zee (2013), A coupled agronomic-economic model to consider allocation of brackish irrigation water, *Water Resour. Res.*, *49*, 2861–2871, doi:10.1002/wrcr.20258.

Bower, C. A., G. Ogata, and J. M. Tucker (1969), Rootzone salt profiles and Alfalfa growth as influenced by irrigation water salinity and leaching fraction, *Agron. J.*, *61*(5), 783–785, doi:10.2134/agronj1969.00021962006100050039x.
Bradford, S., and J. Letey (1992), Cyclic and blending strategies for using nonsaline and saline waters for irrigation, *Irrig. Sci.*, *13*(3), 123–128, doi:10.1007/BF00191054.
Bresler, E., and G. J. Hoffman (1986), Irrigation management for soil salinity control: Theories and tests, *Soil Sci. Soc. Am. J.*, *50*(6), 1552–1560, doi:10.2136/sssaj1986.03615995005000060034x.
Corless, R. M., G. H. Gonnet, D. E. G. Hare, D. J. Jeffrey, and D. E. Knuth (1996), On the LambertW function, *Adv. Comput. Math.*, *5*(1), 329–359, doi:10.1007/BF02124750.
Corwin, D. L., J. D. Rhoades, and J. Simunek (2007), Leaching requirement for soil salinity control: Steady-state versus transient models, *Agric. Water Manage.*, *90*(3), 165–180, doi:10.1016/j.agwat.2007.02.007.
Dinar, A., J. Letey, and K. C. Knapp (1985), Economic evaluation of salinity, drainage and non-uniformity of infiltrated irrigation water, *Agric. Water Manage.*, *10*(3), 221–233, doi:10.1016/0378-3774(85)90013-7.
Ditthakit, P. (2011), Computer software applications for salinity management: A review, *Aust. J. Basic Appl. Sci.*, *5*(7), 1050–1059.
Dudley, L. M., A. Ben-Gal, and U. Shani (2008), Influence of plant, soil, and water on the leaching fraction, *Vadose Zone J.*, *7*(2), 420–425, doi:10.2136/vzj2007.0103.
Falkenmark, M., and J. Rockström (2006), The new blue and green water paradigm: Breaking new ground for water resources planning and management, *J. Water Resour. Plann. Manage.*, *132*(3), 129–132, doi:10.1061/(ASCE)0733-9496(2006)132:3(129).
Feddes, R. A., P. J. Kowalik, and H. Zaradny (1978), *Simulation of Field Water Use and Crop Yield*, Pudoc, Cent. for Agric. Publ. Doc., Wageningen, Netherlands.
Hoffman, G. (1985), Drainage required to manage salinity, *J. Irrig. Drain. Eng.*, *111*(3), 199–206, doi:10.1061/(ASCE)0733-9437(1985)111:3(199).
Hoffman, G. J., and M. Th. van Genuchten (1983), Soil properties and efficient water use: Water management for salinity control, in *Limitations to Efficient Water Use in Crop Production*, edited by H. M. Taylor, W. R. Jordan, and T. R. Sinclair, pp. 73–85, American Society of Agronomy, Madison, Wis.
Kan, I., and M. Rapaport-Rom (2012), Regional blending of fresh and saline irrigation water: Is it efficient? *Water Resour. Res.*, *48*, W07517, doi:10.1029/2011WR011285.
Kan, I., K. A. Schwabe, and K. C. Knapp (2002), Microeconomics of irrigation with saline water, *J. Agric. Resour. Econ.*, *27*(1), 16–39.
Letey, J. (2007), Guidelines for irrigation management of saline waters are overly conservative, in *Wastewater Reuse–Risk Assessment, Decision-Making and Environmental Security*, edited by M. K. Zaidi, pp. 205–218, Springer, Netherlands.
Letey, J., and G. L. Feng (2007), Dynamic versus steady-state approaches to evaluate irrigation management of saline waters, *Agric. Water Manage.*, *91*(1–3), 1–10, doi:10.1016/j.agwat.2007.02.014.
Letey, J., A. Dinar, and K. C. Knapp (1985), Crop-water production function model for saline irrigation waters, *Soil Sci. Soc. Am. J.*, *49*(4), 1005–1009, doi:10.2136/sssaj1985.03615995004900040043x.
Letey, J., G. J. Hoffman, J. W. Hopmans, S. R. Grattan, D. Suarez, D. L. Corwin, J. D. Oster, L. Wu, and C. Amrhein (2011), Evaluation of soil salinity leaching requirement guidelines, *Agric. Water Manage.*, *98*(4), 502–506, doi:10.1016/j.agwat.2010.08.009.
Maas, E. V., and G. J. Hoffman (1977), Crop salt tolerance-current assessment, *J. Irrig. Drain. Div. Am. Soc. Civ. Eng.*, *103*(2), 115–134.
Oster, J. D., J. Letey, P. Vaughan, L. Wu, and M. Qadir (2012), Comparison of transient state models that include salinity and matric stress effects on plant yield, *Agric. Water Manage.*, *103*, 167–175, doi:10.1016/j.agwat.2011.11.011.
Pang, X., and J. Letey (1998), Development and evaluation of ENVIRO-GRO, an integrated water, salinity, and nitrogen model, *Soil Sci. Soc. Am. J.*, *62*(5), 1418–1427.
Raats, P. A. C. (1975), Distribution of salts in the root zone, *J. Hydrol.*, *27*(3–4), 237–248, doi:10.1016/0022-1694(75)90057-8.
Raats, P. A. C. (1981), Residence times of water and solutes within and below the root zone, *Agric. Water Manage.*, *4*(1–3), 63–82, doi:10.1016/0378-3774(81)90044-5.
Rhoades, J. D. (1999), Use of saline drainage water for irrigation, in *Agricultural Drainage*, pp. 615–657, American Society of Agronomy, Madison, Wis.
Schwabe, K. A., I. Kan, and K. C. Knapp (2006), Drainwater management for salinity mitigation in irrigated agriculture, *Am. J. Agric. Econ.*, *88*(1), 133–149, doi:10.1111/j.1467-8276.2006.00843.x.
Shani, U., A. Ben-Gal, E. Tripler, and L. M. Dudley (2007), Plant response to the soil environment: An analytical model integrating yield, water, soil type, and salinity, *Water Resour. Res.*, *43*, W08418, doi:10.1029/2006WR005313.
Shani, U., A. Ben-Gal, E. Tripler, and L. M. Dudley (2009), Correction to "Plant response to the soil environment: An analytical model integrating yield, water, soil type, and salinity," *Water Resour. Res.*, *45*, W05701, doi:10.1029/2009WR008094.
Šimůnek, J., M. Šejna, H. Saito, M. Sakai, and M. Th. van Genuchten (2013), *The HYDRUS-1D Software Package for Simulating the Movement of Water, Heat, and Multiple Solutes in Variably Saturated Media, Version 4.17, HYDRUS Software Ser. 3*, Dep. of Environ. Sci., Univ. of Calif. Riverside, Riverside.
Skaggs, T. H., M. T. van Genuchten, P. J. Shouse, and J. A. Poss (2006), Macroscopic approaches to root water uptake as a function of water and salinity stress, *Agric. Water Manage.*, *86*(1–2), 140–149, doi:10.1016/j.agwat.2006.06.005.
Skaggs, T. H., N. J. Jarvis, E. M. Pontedeiro, M. T. van Genuchten, and R. M. Cotta (2007), Analytical advection-dispersion model for transport and plant uptake of contaminants in the root zone, *Vadose Zone J.*, *6*(4), 890–898, doi:10.2136/vzj2007.0124.
Skaggs, T. H., D. L. Suarez, and S. Goldberg (2013), Effects of soil hydraulic and transport parameter uncertainty on predictions of solute transport in large lysimeters, *Vadose Zone J.*, *12*(1), doi:10.2136/vzj2012.0143.
Skaggs, T. H., D. L. Suarez, and D. L. Corwin (2014), Global sensitivity analysis for UNSATCHEM simulations of crop production with degraded waters, *Vadose Zone J.*, *13*(6), doi:10.2136/vzj2013.09.0171.
Steppuhn, H., M. Th. van Genuchten, and C. M. Grieve (2005), Root-zone salinity, *Crop Sci.*, *45*(1), 221–232, doi:10.2135/cropsci2005.0221.
Strzepek, K., and B. Boehlert (2010), Competition for water for the food system, *Philos. Trans. R. Soc. B*, *365*(1554), 2927–2940, doi:10.1098/rstb.2010.0152.
Suarez, D., and J. Simunek (1997), UNSATCHEM: Unsaturated water and solute transport model with equilibrium and kinetic chemistry, *Soil Sci. Soc. Am. J.*, *61*(6), 1633–1646.
Suarez, D. L. (2012), Modeling transient root zone salinity (SWS model), in *Agricultural Salinity Assessment and Management*, vol. 71, edited by W. W. Wallender and K. K. Tanji, pp. 855–897, Am. Soc. of Civ. Eng., Reston, Va.
U.S. Salinity Laboratory Staff (1954), *Diagnosis and Improvement of Saline and Alkali Soils, U.S. Department of Agriculture Handbook*, vol. 60, U.S. Gov. Print. Off., Washington, D. C.

van Dam, J. C., P. Groenendijk, R. F. A. Hendriks, and J. G. Kroes (2008), Advances of modeling water flow in variably saturated soils with SWAP, *Vadose Zone J.*, *7*, 640–653, doi:10.2136/vzj2007.0060.

van Genuchten, M. Th., and S. K. Gupta (1993), A reassessment of the crop tolerance response function, *J. Indian Soc. Soil Sci.*, *41*, 730–737.

Vinten, A. J. A., H. Frenkel, J. Shalhevet, and D. A. Elston (1991), Calibration and validation of a modified steady-state model of crop response to saline water irrigation under conditions of transient root zone salinity, *J. Contam. Hydrol.*, *7*(1–2), 123–144, doi:10.1016/0169-7722(91)90041-X.

Weisstein, E. W. (2014), *Cubic Formula* [online], MathWorld—A Wolfram Web Resour. [Available at http://mathworld.wolfram.com/CubicFormula.html.]

Wolfram Research, Inc. (2008), *Mathematica*, Wolfram Res., Champaign, Ill [Available at http://mathworld.wolfram.com/about/faq.html#citation.]